View metadata, citation and similar papers at core.ac.uk
brought to you by CORE
provided by Directory of Open Access Journals

THERMAL BUCKLING ANALYSIS OF LAMINATED COMPOSITE PLATES USING EDGE-BASED SMOOTHED DISCRETE SHEAR GAP METHOD

by Tran Vinh Loc[1], Phan Dao Hoang Hiep[2], Nguyen Xuan Hung[3]

ABSTRACT

In this paper, we analyze a thermal buckling behavior of laminated composite plates based on first-order shear deformation theory (FSDT) using edge-based smoothed discrete shear gap method (ES–DSG). In the ES-DSG, only the linear approximation is necessary and the discrete shear gap method (DSG) for triangular plate elements is used to avoid the shear locking and spurious zero energy modes. In addition, the stiffness matrices are computed based on smoothing domains created by connecting two end-nodes of the edge to centroids of adjacent triangular elements. The temperature in the plates is assumed to be uniform distribution and rise. Several numerical examples are given to verify the reliability of the obtained results compared to other published solutions.

Keywords: Laminated composite plates, edge-based smoothed finite element method (ES-FEM), first-order shear deformation theory (HSDT), thermal buckling.

1. INTRODUCTION

Composite materials have been widely used in many engineering such as aerospace, marine, buildings, etc. because of many favorable mechanical properties such as strength-to-weight ratios, long fatigue life, wear resistance, damping, etc. [1]. It means that to ensure the strength capacity the composite material is used with thinner and slighter than traditional material. It helps to decrease the weight of structure, to keep smaller shape and to save materials. However, besides the results from study of static and dynamic problems, the buckling analysis needs to take care. Because of some cases as thin wall structures as plates and shell subjected to in-plane compressible force, the structures can be buckled before reaching to yield stress. The structures have large deformation and lose load carrying capacity. The buckling state can be divided two types: Mechanical buckling by mechanical loads and thermal buckling by the temperature rise.

Up to now, many researches on thermal buckling problem of composite plates have been found in the literature based on many approaches and various plate theories. In order to improve the accuracy of transverse shear stresses when composite plates become thicker and more lamina layers, layer-wise (LW) model has been developed. Typically, M. Shariyat [2] used the finite element method combined with the layer-wise theory to solve thermal buckling analysis of rectangular composite plates under temperature - dependent

[1]*Division of Computational Mechanics, Ton Duc Thang University Ho Chi Minh City.*

[2]*Faculty of Civil Engineering, Ton Duc Thang University Ho Chi Minh City.*

[3]*Department of Mechanics, Faculty of Mathematics and Computer Science, University of Science Ho Chi Minh City.*

properties. However, this work took much computational cost. Hence, another model widely developed with simplicity in formulating constitutive equations and lower computational cost was so-called Equivalent Single-Layer (ESL) model. Herein, the strain fields were expressed based on many plate theories. The simplest one named the Classical Laminated Plate Theory (CLPT) is applied to determine the critical temperature parameter of angle-ply laminated plates under uniform temperature by Gossard [3]. However, the CLPT using the Love-Kirchhoff assumptions is inadequate for the analysis of thick laminated composite plates, and hence the First-order Shear Deformation Theory which takes into account the effects of shear deformation has been developed. Tauchert [4] used FSDT to present an exact thermal buckling solution of angle-ply laminated plates subjected to a uniform rise. W. J. Chen [5] used FEM to study the effects of lamination angle, modulus ratio, plate aspect ratio, and boundary constrains of thick composite laminated plates under non-uniform temperature distribution. To enhance the accuracy of solutions, High-order Shear Deformation Theory (HSDT) was used and applied for thermal buckling analyses of cross-ply/angle-ply laminated and sandwich plates by H. Matsunaga [6, 7]. However, HSDT requires C^1-continuity of generalized displacements or needs much unknown variables to approximate displacement field. In addition, it is quite the difficulty and high computational cost for formulating and modeling. The FSDT of ELS is thus focused in this paper.

This paper deals with thermal buckling analysis of laminated composite plates based on first-order shear deformation theory (FSDT) using edge-based smoothed finite element method (ES–FEM). In the ES–FEM, the edge-based strain smoothing techniques are performed over smoothing domains associated with the edges of the triangular elements to achieve "efficiently softer" stiffness matrices. Due to using linear approximations, the formulations become simple and it has no requirement of high computational cost. Several numerical examples are used to verify the reliability of the method compared to other published models.

2. PROBLEM FORMULATION

2.1. Theoretical formulation

Let consider a laminated composite plate with length a, width b and thickness h, the stress-strain relative equations of k^{th} layer were shown below:

$$\boldsymbol{\sigma} = \mathbf{Q}\left(\boldsymbol{\varepsilon} - \boldsymbol{\varepsilon}_t\right) \tag{1}$$

Considering α_{11}, α_{22} are the thermal expansion coefficients along the material coordinate system (x_1, x_2) and following the tensor transformation rule [1], these terms become (α_x, α_y, α_{xy}) in global coordinate system.

In the global coordinate system, the constitutive relation can be expressed:

$$\begin{Bmatrix} \sigma_x \\ \sigma_y \\ \tau_{xy} \\ \tau_{yz} \\ \tau_{xz} \end{Bmatrix} = \begin{bmatrix} \bar{Q}_{11} & \bar{Q}_{12} & \bar{Q}_{16} & 0 & 0 \\ \bar{Q}_{12} & \bar{Q}_{22} & \bar{Q}_{26} & 0 & 0 \\ \bar{Q}_{16} & \bar{Q}_{26} & \bar{Q}_{66} & 0 & 0 \\ 0 & 0 & 0 & \bar{Q}_{44} & \bar{Q}_{45} \\ 0 & 0 & 0 & \bar{Q}_{45} & \bar{Q}_{55} \end{bmatrix} \begin{Bmatrix} \varepsilon_x - \alpha_x \Delta T \\ \varepsilon_y - \alpha_y \Delta T \\ \gamma_{xy} - 2\alpha_{xy} \Delta T \\ \gamma_{yz} \\ \gamma_{xz} \end{Bmatrix} \tag{2}$$

Based on the FSDT, the displacement field $\mathbf{u} = [u \;\; v \;\; w]^T$ can be expressed as [1]:

$$\begin{cases} u(x,y,z) = u_0 + z\theta_x \\ v(x,y,z) = v_0 + z\theta_y \\ w(x,y,z) = w_0 \end{cases} \quad (3)$$

where (u_0, v_0, w_0) are the mid-plane displacements of a point along the (x, y, z) coordinate direction, respectively, z is the distance from the mid-plane to the point considered and (θ_x, θ_y) denote the transverse rotations about the y,x axes, respectively.

The strain-displacement relation of linear elasticity can be written as:

$$\boldsymbol{\varepsilon} = \begin{Bmatrix} \boldsymbol{\varepsilon}^0 \\ 0 \end{Bmatrix} + \begin{Bmatrix} z\boldsymbol{\kappa}_b \\ \boldsymbol{\gamma} \end{Bmatrix} \quad (4)$$

where $\boldsymbol{\varepsilon}^0, \boldsymbol{\kappa}_b, \boldsymbol{\gamma}$ are the membrane, bending strain and transverse shear, respectively.

$$\boldsymbol{\varepsilon}^0 = \begin{Bmatrix} \varepsilon_x^m \\ \varepsilon_y^m \\ \gamma_{xy}^m \end{Bmatrix} = \begin{Bmatrix} u_{0,x} \\ v_{0,y} \\ u_{0,y} + v_{0,x} \end{Bmatrix} \quad , \quad \boldsymbol{\kappa}_b = \begin{Bmatrix} \varepsilon_x^b \\ \varepsilon_y^b \\ \gamma_{xy}^b \end{Bmatrix} = \begin{Bmatrix} \theta_{x,x} \\ \theta_{y,y} \\ \theta_{x,y} + \theta_{y,x} \end{Bmatrix} \quad , \quad \boldsymbol{\gamma} = \begin{Bmatrix} \gamma_{xz} \\ \gamma_{yz} \end{Bmatrix} = \begin{Bmatrix} \theta_x + w_{,x} \\ \theta_y + w_{,y} \end{Bmatrix} \quad (5)$$

The stress resultants ***N,Q*** and moment resultants ***M*** can be obtained:

$$\boldsymbol{N} = \begin{Bmatrix} N_x \\ N_y \\ N_{xy} \end{Bmatrix} = \int_{-h/2}^{h/2} \begin{Bmatrix} \sigma_x \\ \sigma_y \\ \sigma_{xy} \end{Bmatrix} dz \quad , \quad \boldsymbol{Q} = \begin{Bmatrix} Q_x \\ Q_y \end{Bmatrix} = \int_{-h/2}^{h/2} \begin{Bmatrix} \sigma_{xz} \\ \sigma_{yz} \end{Bmatrix} dz \quad , \quad \boldsymbol{M} = \begin{Bmatrix} M_x \\ M_y \\ M_{xy} \end{Bmatrix} = \int_{-h/2}^{h/2} \begin{Bmatrix} \sigma_x \\ \sigma_y \\ \sigma_{xy} \end{Bmatrix} zdz \quad (6)$$

The integration form of stresses through thickness of laminated plates is

$$\begin{bmatrix} \boldsymbol{N} \\ \boldsymbol{M} \\ \boldsymbol{Q} \end{bmatrix} = \begin{bmatrix} \mathbf{A} & \mathbf{B} & \mathbf{0} \\ \mathbf{B} & \mathbf{D} & \mathbf{0} \\ \mathbf{0} & \mathbf{0} & \mathbf{C} \end{bmatrix} \begin{Bmatrix} \boldsymbol{\varepsilon}^0 \\ \boldsymbol{\kappa}_b \\ \boldsymbol{\gamma} \end{Bmatrix} - \begin{bmatrix} \boldsymbol{N}_t \\ \boldsymbol{M}_t \\ \mathbf{0} \end{bmatrix} \quad (7)$$

where (**A, B, D**) are the extensional stiffness, bending-extensional coupling and bending stiffness, respectively. The terms of lamina stiffness are defined as:

$$(\mathbf{A},\mathbf{B},\mathbf{D}) \equiv \left(A_{ij}, B_{ij}, D_{ij}\right) = \int_{-h/2}^{h/2} \left(1, z^2, z^4\right) \bar{Q}_{ij} \mathrm{d}z \qquad i,j = 1,2,6 \quad (8)$$

$$\mathbf{C} \equiv C_{ij} = \int_{-h/2}^{h/2} \mu \bar{Q}_{ij} \mathrm{d}z \qquad i,j = 4,5 \quad (9)$$

in which, $\mu = 5/6$ is shear correction factor.

Thermal stress resultants $\boldsymbol{N}_t$ and thermal moment resultants $\boldsymbol{M}_t$ can be expressed as:

$$\boldsymbol{N}_t = \begin{Bmatrix} N_{tx} \\ N_{ty} \\ N_{txy} \end{Bmatrix} = \int_{-h/2}^{h/2} \overline{Q}_{ij} \begin{Bmatrix} \alpha_x \\ \alpha_y \\ 2\alpha_{xy} \end{Bmatrix} \Delta T dz \quad , \quad \boldsymbol{M}_t = \begin{Bmatrix} M_{tx} \\ M_{ty} \\ M_{txy} \end{Bmatrix} = \int_{-h/2}^{h/2} \overline{Q}_{ij} \begin{Bmatrix} \alpha_x \\ \alpha_y \\ 2\alpha_{xy} \end{Bmatrix} \Delta T z dz \tag{10}$$

where ΔT is the temperature rise.

2.2. Brief on FEM formulation

The problem domain is divided into N_e finite triangular elements with N_n nodes. The displacement field $\mathbf{u}^h$ was approximated as [8, 9]:

$$\mathbf{u}^h = \sum_{I=1}^{N_n} \mathbf{N}_I(\mathbf{x})\mathbf{d}_I \tag{11}$$

where $\mathbf{N}$ is the matrix of shape functions, $\mathbf{d}_I = \begin{bmatrix} u_{0I} & v_{0I} & w_{0I} & \theta_{xI} & \theta_{yI} \end{bmatrix}^T$ is the nodal degree-of-freedom associated with node I.

The membrane, bending and shear strains can be expressed as:

$$\boldsymbol{\varepsilon}^0 = \sum_I \mathbf{B}_I^m \mathbf{d}_I \quad , \quad \boldsymbol{\kappa}_b = \sum_I \mathbf{B}_I^b \mathbf{d}_I \quad , \quad \boldsymbol{\gamma} = \sum_I \mathbf{B}_I^s \mathbf{d}_I \tag{12}$$

According to the finite element method (FEM), total potential energy can be expressed as [5]:

$$\boldsymbol{\Pi} = \sum_{i=1}^{N_e} \boldsymbol{\Pi}_i = \sum_{i=1}^{N_e} \left[\frac{1}{2}\left(\mathbf{d}_i^e\right)^T \mathbf{K}^e \mathbf{d}_i^e - \left(\mathbf{d}_i^e\right)^T \mathbf{F}_t^e + \frac{1}{2}\left(\mathbf{d}_i^e\right)^T \mathbf{K}_g^e \mathbf{d}_i^e \right] = \frac{1}{2}\mathbf{d}^T \mathbf{K} \mathbf{d} - \mathbf{d}^T \mathbf{F}_t + \frac{1}{2}\mathbf{d}^T \mathbf{K}_g \mathbf{d} \tag{13}$$

in which the stiffness matrix:

$$\mathbf{K}^e = \int_\Omega \left[\left(\mathbf{B}^m\right)^T \mathbf{A}\mathbf{B}^m + \left(\mathbf{B}^m\right)^T \mathbf{B}\mathbf{B}^b + \left(\mathbf{B}^b\right)^T \mathbf{B}\mathbf{B}^m + \left(\mathbf{B}^b\right)^T \mathbf{D}\mathbf{B}^b + \left(\mathbf{B}^s\right)^T \mathbf{C}\mathbf{B}^s \right] d\Omega \tag{14}$$

and the geometric stiffness matrix:

$$\mathbf{K}_g^e = \int_\Omega \left[\left(\mathbf{B}^g\right)^T \boldsymbol{N}_0 \mathbf{B}^g \right] d\Omega \tag{15}$$

and the thermal load vector:

$$\mathbf{F}_t^e = \int_\Omega \left[\left(\mathbf{B}^t\right)^T \boldsymbol{N}_t + \left(\mathbf{B}^b\right)^T \boldsymbol{M}_t \right] d\Omega \tag{16}$$

$$\boldsymbol{N}_0 = \begin{bmatrix} N_x & N_{xy} \\ N_{xy} & N_y \end{bmatrix} \tag{17}$$

Let minimize Eq.(13) with respect to the generalized displacement vector yielding the linear static equation [5]:

$$\mathbf{K}\mathbf{d} = \mathbf{F}_t \tag{18}$$

For critical buckling state, the second minimization of total potential energy can be obtained as [12]:

$$\left|\mathbf{K} + \lambda \mathbf{K}_g\right| = 0 \tag{19}$$

The multiplication of parameter λ and the initial temperature ΔT is the critical buckling temperature T_{cr}:

$$T_{cr} = \lambda \Delta T \tag{20}$$

2.3. The formulation of ES-FEM with stabilized discrete shear gap (DSG) technique

The linear triangular elements often occur shear locking problem when the thickness decreases to limit of thin plate. To alleviate this shortcoming, Bletzinger *et al.* (2000) [10] have proposed the discrete shear gap method (DSG). As a result, the transverse shear strain was obtained becoming constants and avoids shear locking phenomena:

$$\mathbf{B}^s_{DSG3} = \frac{1}{2A_e}\begin{bmatrix} 0 & 0 & b-c & A_e & 0 & 0 & 0 & c & ac/2 & bc/2 & 0 & 0 & -b & -bd/2 & -bc/2 \\ 0 & 0 & d-a & 0 & A_e & 0 & 0 & -d & -ad/2 & -bd/2 & 0 & 0 & a & ad/2 & ac/2 \end{bmatrix} \tag{21}$$

where $a = x_2 - x_1, b = y_2 - y_1, c = y_3 - y_1, d = x_3 - x_1$ and $A_e = ac - bd$ is the area of 3-node element.

In development of improved accuracy of linear triangular elements, Nguyen-Xuan *et al*. [8] developed an edge-based strain smoothing technique into the DSG FEM to give a so-called edge-based smoothed discrete shear gap method (ES-DSG). In formulation of ES-DSG, the strains are "smoothed" over smoothing domains $\Omega^{(k)}$ associated with edges of the elements such that $\Omega = \bigcup_k^{N_{ed}} \Omega^{(k)}$ and $\Omega^{(i)} \cap \Omega^{(j)} = \varnothing$ with $i \neq j$, in which N_{ed} is the total number of edges in the entire problem domain. The smoothing domain $\Omega^{(k)}$ associated with the edge k is created by connecting two end-nodes of the edge to centroids of adjacent elements as shown in Figure 1.

The smoothed strains over the smoothing domain $\Omega^{(k)}$ can be obtained as:

$$\tilde{\boldsymbol{\varepsilon}}_k = \int_{\Omega^{(k)}} \boldsymbol{\varepsilon}^h(\mathbf{x})\Phi(\mathbf{x})d\Omega \tag{22}$$

where Φ(x) is a smoothing function that is positive and satisfies unity condition:

$$\int_{\Omega^{(k)}} \Phi(\mathbf{x})d\Omega = 1 \quad \text{and in the simplicity form:} \quad \Phi(\mathbf{x}) = \begin{cases} 1/A^{(k)} & ,\mathbf{x} \in \Omega^{(k)} \\ 0 & ,\mathbf{x} \notin \Omega^{(k)} \end{cases} \tag{23}$$

Figure 1. Division of domain into triangular element and smoothing cells $\Omega^{(k)}$ connected to edge k

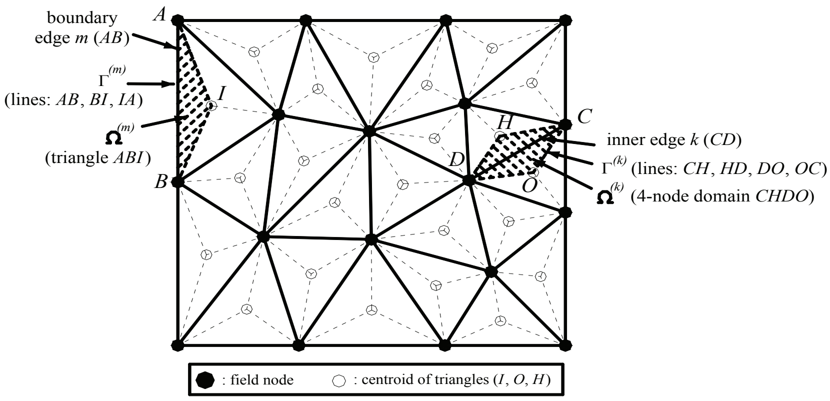

Substitute Eq. (23) into Eq. (22), the smoothed strains of the ES-DSG3 become:

$$\tilde{\boldsymbol{\varepsilon}}_k^h = \frac{1}{A^{(k)}}\int_{\Omega^{(k)}} \boldsymbol{\varepsilon}^h d\Omega \tag{24}$$

where $A^{(k)}$ is the area of the smoothing cell $\Omega^{(k)}$ and defined as:

$$A^{(k)} = \int_{\Omega^{(k)}} d\Omega = \frac{1}{3}\sum_{i=1}^{N_e^{(k)}} A_i \tag{25}$$

where $N_e^{(k)}$ is the number of elements containing the edge k ($N_e^{(k)} = 1$ for the boundary edges and $N_e^{(k)} = 2$ for inner edges) and A_i is the area of the i^{th} element around the edge k.

The average strains according to edge k can be obtained as following form by substituting Eq.(12) and Eq.(21) into Eq.(24):

$$\boldsymbol{\varepsilon}^0 = \sum_{I=1}^{N_n^{(k)}} \tilde{\mathbf{B}}_I^m \mathbf{d}_I \quad , \quad \boldsymbol{\kappa}_b = \sum_{I=1}^{N_n^{(k)}} \tilde{\mathbf{B}}_I^b \mathbf{d}_I \quad , \quad \boldsymbol{\gamma} = \sum_{I=1}^{N_n^{(k)}} \tilde{\mathbf{B}}_I^s \mathbf{d}_I \tag{26}$$

where $N_n^{(k)}$ is the number of nodes belonging to elements directly connected to edge k ($N_n^{(k)} = 3$ for the boundary edges and $N_n^{(k)} = 4$ for inner edges).

Due to linear approximated functions were used in the triangular elements, the matrices of smoothed gradient strains are constants and can be expressed as:

$$\tilde{\mathbf{B}}_I^m = \frac{1}{A^{(k)}}\sum_{i=1}^{N_e^{(k)}} A_i\,\mathbf{B}_i^m \quad , \quad \tilde{\mathbf{B}}_I^b = \frac{1}{A^{(k)}}\sum_{i=1}^{N_e^{(k)}} A_i\,\mathbf{B}_i^b \quad , \quad \tilde{\mathbf{B}}_I^s = \frac{1}{A^{(k)}}\sum_{i=1}^{N_e^{(k)}} A_i\,\mathbf{B}_i^{sDSG3} \tag{27}$$

As a result, the mechanical stiffness matrix of global coordinate system can be obtained as:

$$\tilde{\mathbf{K}} = \sum_{k=1}^{N_{ed}} \tilde{\mathbf{K}}^{(k)} \tag{28}$$

where

$$\tilde{\mathbf{K}}^{(k)} = \int_{\Omega^{(k)}} \left[\left(\tilde{\mathbf{B}}^m\right)^T \mathbf{A}\tilde{\mathbf{B}}^m + \left(\tilde{\mathbf{B}}^m\right)^T \mathbf{B}\tilde{\mathbf{B}}^b + \left(\tilde{\mathbf{B}}^b\right)^T \mathbf{B}\tilde{\mathbf{B}}^m + \left(\tilde{\mathbf{B}}^b\right)^T \mathbf{D}\tilde{\mathbf{B}}^b + \left(\tilde{\mathbf{B}}^s\right)^T \mathbf{C}\tilde{\mathbf{B}}^s \right] d\Omega$$
$$= \left[\left(\tilde{\mathbf{B}}^m\right)^T \mathbf{A}\tilde{\mathbf{B}}^m + \left(\tilde{\mathbf{B}}^m\right)^T \mathbf{B}\tilde{\mathbf{B}}^b + \left(\tilde{\mathbf{B}}^b\right)^T \mathbf{B}\tilde{\mathbf{B}}^m + \left(\tilde{\mathbf{B}}^b\right)^T \mathbf{D}\tilde{\mathbf{B}}^b + \left(\tilde{\mathbf{B}}^s\right)^T \mathbf{C}\tilde{\mathbf{B}}^s \right] A^{(k)} \quad (29)$$

It can be seen that the stiffness matrix are constants and can be easily computed by straight-forward integration.

3. NUMMERICAL RESULTS

In this section, the ES-DSG3 element is used to analyze thermal buckling behavior of laminated composite plates. Thin plates and moderate thick ones are considered with influence of some parameters such as modulus property ratio, span-to-thickness ratio, boundary condition, stacking sequence, and fiber orientation. Computer programs have been developed to calculate present solutions through the number of numerical examples.

3.1. Isotropic square plate

First, we consider an isotropic plate *a/h=100* which has following material properties $E=1,\ \nu=0.3,\ \alpha=1\times10^{-6}\left({}^{0}\mathrm{C}^{-1}\right)$ and subjected to uniform temperature rise. The present results are compared with the analytical solution reported in Boley [11] and the numerical solution by Chen et al. [5] which used FEM-Q8 based on FSDT.

Table 1: Simply supported isotropic plate with various *a/b* ratios: Critical buckling temperature.

a/b	T_{cr}		
	Ref [11]	Q8/FSDT [5]	Present
0.25	0.686	0.691	0.689
0.5	0.808	0.814	0.812
1.0	1.283	1.319	1.287
1.5	2.073	2.101	2.096
2.0	3.179	3.191	3.233
2.5	4.599	4.601	4.689
3.0	6.332	6.330	6.449

Figure 2. Percentages of critical temperature errors of simply supported isotropic plate with various *a/b* ratios (*a*/h=100).

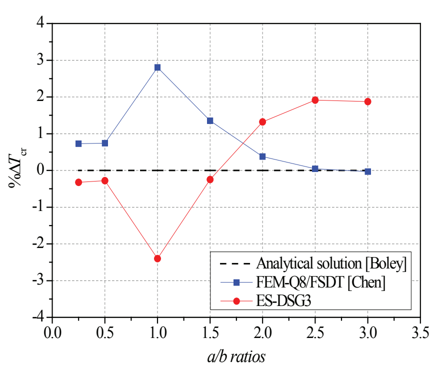

It can be seen from Table 1 that the results of the ES-DSG3 have good agreement with available ones. Note that the present method just using linear approximation not only passes shear-locking phenomena but also can produce the accuracy of the solutions similar to the high-order element such as FEM-Q8. In Figure 2, the percentages of critical temperature error are relatively small (<2.5%).

3.2. Laminated composite plates

The simply supported 4-layer $[0^0/90^0/90^0/0^0]$ square laminated composite plates are considered. The material properties are given as:

$$\begin{aligned}&E_1/E_2=15, \quad E_3=E_2, \quad G_{12}/E_2=G_{13}/E_2=0.5, \quad G_{23}/E_2=0.3356,\\&\nu_{12}=\nu_{13}=0.3, \quad \nu_{23}=0.49, \quad \alpha_1/\alpha_0=0.015, \quad \alpha_2/\alpha_0=\alpha_3/\alpha_0=1.0, \quad \alpha_0=10^{-6}\left({}^0\mathrm{C}^{-1}\right)\end{aligned} \tag{30}$$

The effects of boundary conditions on thermal buckling behavior are displayed in the Table 2. The results obtained are compared with those of high-order element (FEM-Q16 with 3x3 Gauss points for shear terms and 4x4 for others) based on FSDT and HSDT [12]. It can be seen that the present results match well with those of FEM-Q16/FSDT.

Table 2: Critical buckling temperature of symmetric cross-ply $[0^0/90^0/90^0/0^0]$ laminated composite plate with various boundary conditions (*a/h* = 100).

Boundary conditions	$T_{cr}\times 10^2$			
	SSSS	CSCS	SCSC	CCCC
ES-DSG3 (20x20 mesh)/FSDT	0.09976 (0.16%)	0.14488 (0.61%)	0.25261 (-0.15%)	0.33996 (1.54%)
FEM-Q16 (6x6 mesh)/FSDT [12]	0.0997	0.1441	0.2532	0.3352
FEM-Q16 (6x6 mesh)/HSDT [12]	0.0996	0.1440	0.2530	0.3348

“S” denoted simply supported and “C” denoted clamped.

“CSCS” denoted straight edges clamped and perpendicular edges simply supported and “SCSC” the same.

Table 3: Critical buckling temperature of symmetric cross-ply $[0^0/90^0/90^0/0^0]$ laminated composite plate with various boundary conditions (*a/h* = 100).

Boundary conditions	T_{cr}			
	SSSS	CSCS	SCSC	CCCC
ES-DSG3 (20x20 mesh)/FSDT	0.07605 (-1.23%)	0.10842 (1.42%)	0.13745 (2.27%)	0.16888 (2.04%)
Q16 (6x6 mesh)/FSDT [12]	0.0770	0.1069	0.1344	0.1655
Q16 (6x6 mesh)/HSDT [12]	0.0757	0.1044	0.1305	0.1601

Table 3 shows the critical temperature parameter for moderate thick symmetric cross-ply $[0^0/90^0/90^0/0^0]$ laminated composite plate with span-to-thickness ratio $a/h = 10$. The influence of boundary condition over symmetric plates can be remarked that when the boundary condition of plate becomes harder, the value of the critical temperature increases. Using triangular meshes with linear interpolation, the present method shows good agreement with the high-order element (Q16) and does not take much computational cost.

It can be seen that the ES-DSG3 is well suited for thin or moderate thick symmetric laminated composite plates. Next, anti-symmetric angle-ply $[45^0/-45^0/\ldots]$ laminate plates with influence of stacking sequence are considered. The number of layers (*NL*) is equal to 4 and 10, respectively. The percentages of the error presented in Table 4 are almost under 1% compared with FEM-Q16/FSDT solutions [12].

Table 4: Critical buckling temperature of anti-symmetric angle-ply $[45^0/-45^0/\ldots]$ laminated composite plate with various boundary conditions ($a/h = 100$).

Boundary conditions	$T_{cr} \times 10^2$			
	SSSS	CSCS	SCSC	CCCC
NL = 4				
ES-DSG3 (20x20 mesh)/FSDT	0.14615 (-0.51%)	0.23161 (-0.34%)	0.23161 (-0.34%)	0.30312 (-0.29%)
Q16 (6x6 mesh)/FSDT [12]	0.1469	0.2324	0.2324	0.3040
Q16 (6x6 mesh)/HSDT [12]	0.1468	0.2322	0.2322	0.3036
NL = 10				
ES-DSG3 (20x20 mesh)/FSDT	0.16365 (-2.30%)	0.26541 (0.65%)	0.26541 (0.65%)	0.34750 (0.96%)
Q16 (6x6 mesh)/FSDT [12]	0.1675	0.2637	0.2637	0.3442
Q16 (6x6 mesh)/HSDT [12]	0.1675	0.2637	0.2637	0.3441

4. CONCLUSION

Based on the C^0–type first-order shear deformation theory and the edge-based smoothed discrete shear gap method (ES-DSG3), thermal buckling behavior of laminated composite plates has been studied in this paper. The stiffness matrices are simply obtained by smoothing strain terms over smoothing domains associated with the edges. The performances of the ES-DSG3 element were shown through various numerical examples. Some advantages of this element can be noted such as (1) the results mark well with analytical solutions and other published issues in the literature; (2) it does not require high-order derivation of shape function because the linear approximations were used; and (3) the formulation is easily integrated compared to standard FEM. The present method is thus promising to provide a useful tool for thermal buckling analysis of laminated plates.

REFERENCES

1. J.N. Reddy. Mechanics of laminated composite plates-theory and analysis. NewYork: CRC Press;1997.
2. M. Shariyat. Thermal buckling analysis of rectangular composite plates with temperature-dependent properties based on a layerwise theory. Thin-Walled Structures 45 (2007) 439-452.
3. Gossard M. L., Seide P., Roberts W. M. Thermal buckling of plates. NACA TND 1952:2771.
4. T. R. Tauchert. *Thermal buckling of thick antisymmetric angle-ply laminates.* J. Thermal Stresses 10 (1987) 113-124.
5. W. J. Chen, P. D. Lin, L. W. Chen. Thermal buckling behavior of thick composite laminated plates under nonuniform temperature distribution. Computers & Structures Vol 41, No. 4 (1991) 637-645.
6. Hiroyuki Matsunaga. Thermal buckling of cross-ply laminated composite and sandwich plates according to a global higher-order deformation theory. Composite Structures 68 (2005) 439-454.
7. Hiroyuki Matsunaga. Thermal buckling of angle-ply laminated composite and sandwich plates according to a global higher-order deformation theory. Composite Structures 72:2 (2006) 177-192.
8. H. Nguyen-Xuan, G.R. Liu, C. Thai-Hoang, T. Nguyen-Thoi. An edge-based smoothed finite element method (ES-FEM) with stabilized discrete shear gap technique for analysis of Reissner–Mindlin plates. Comput. Methods Appl. Mech. Engrg. Vol 199 (2010) 471-489.
9. H. Nguyen-Xuan, Loc V. Tran, T. Nguyen-Thoi, H.C Vu Do, *Analysis of functionally graded plates using an edge-based smoothed finite element method*, Composite Structures, in press, doi:10.1016/j.compstruct.2011.04.028, 2011.
10. Bletzinger KU, Bischoff M, Ramm E. A unified approach for shear-locking free triangular and rectangular shell finite elements. Comput Struct 75 (2000) 321–34.
11. B. A. Boley and J. J. Weiner. Theory of thermal stress, John Wiley, New York (1960).
12. Kant T., Babu C. S. Thermal buckling analysis of skew fibre-reinforced composite and sandwich plates using shear deformable finite element models. Computers & Structures Vol 49, No. 1 (2000) 77-85.